Journal of Renewable Materials

Tech Science Press

DOI: 10.32604/jrm.2022.022972

check for updates

ARTICLE

Nano-CaO_2 Promotes the Release of Carbon Sources from Municipal Sludge and the Preparation of Double-Network Hydrogels with High Swelling Ratios

Yalin Li[1,2,*], Yu Huang[2], Lei Liu[1], Haozhao Liu[1], Haiyang He[1], Dongxue Lu[1] and Tingting Dong[1]

[1]School of College of Environmental and Biological Engineering, Henan University of Engineering, Zhengzhou, 451191, China

[2]School of Civil Engineering, Architecture and Environment, Hubei University of Technology, Wuhan, 430068, China

[*]Corresponding Author: Yalin Li. Email: li_ya_lin@haue.edu.cn

Received: 03 April 2022 Accepted: 06 June 2022

ABSTRACT

In this study, hydrogels were prepared from municipal sludge to recycle and realize the value-added utilization of the carbon components in this abundant waste material. The carbon sources were extracted from the municipal sludge using synthesised nano CaO_2 as an oxidant, and the carbon sources were graft copolymerised with acrylic acid monomer using N, N′-methylenebisacrylamide as a crosslinking agent and ammonium persulfate as an initiator. The factors influencing the hydrogel preparation were investigated by single-factor experiments. Based on the results of the single-factor experiments, a hydrogel with a swelling ratio of up to 19768.4% at 12 h was prepared with an oxidant dosage of 0.20 g, a monomer dosage of 5.8 g, a neutralisation degree of the monomer of 70%, an initiator dosage of 0.15 g, and a crosslinking agent dosage of 0.15 g. The hydrogel preparation conditions were optimized using the response surface method, and the interactions between the different reaction conditions were analysed to obtain the best preparation conditions. X-ray diffraction results showed that hydrogels were amorphous in structure. Scanning electron microscopy images showed that the SiO_2 particles from the sludge acted as crosslinking points between different layers of hydrogel chains. The crosslinking polymerisation and crosslinking agent worked together to form hydrogels with an inorganic-organic double network structure, and this structure was highly stretchable, resulting in hydrogels with good swelling properties.

KEYWORDS

Oxidant; municipal sludge; carbon component; swelling property; hydrogel

1 Introduction

The production of domestic sewage is rapidly rising as urbanization in China accelerates. Municipal sludge (MS) is a by-product of sewage treatment process and is associated with various environmental problems if it is not properly treated and disposed [1]. At present, the most widely used treatment methods include incineration, disposal in landfills, composting, and production of building materials [2]. However, all of these treatment technologies emit CO_2 or CH_4 as well as other greenhouse gases into the environment, causing secondary pollution and wasting the carbon resources in MS [3]. With the goals of mitigating the "carbon peak" and achieving "carbon neutrality" in China, the efficient utilisation of MS is an immediate challenge that needs to be solved in the field of environmental protection.

Hydrogels are a class of highly-functional polymeric materials that not only have unique three-dimensional crosslinked structures with soft textures that maintains their specific shapes, but also are highly absorbent, have good biocompatibility and biodegradability, and are environmentally friendly and economically renewable in a wide range of applications such as agriculture, landscape, and environmental governance [4]. For example, Cheng et al. [5] prepared a highly absorbent hydrogel using acrylic acid and urea as monomers, potassium persulfate as an initiator and MBA as a crosslinking agent that could be used for the sustained release of nitrogen fertilizer in agricultural applications. Peng et al. [6] prepared novel porous hydrogels by graft copolymerisation of acrylic acid and xylan-rich hemicelluloses and used these materials to absorb heavy metal ions, including Zn^{2+}, Cd^{2+} and Pd^{2+} from wastewater. Wang et al. [7] applied a highly absorbent hydrogel to soil and found that the hydrogel improved the porous network structure of the soil as well as enhanced the water retention in the soil to a certain extent. As a result, the added hydrogels improved crop yields and played a positive role in agricultural production. However, hydrogels also have several disadvantages including they have low mechanical strengths, are poorly durable, and are easily broken under long-term swelling or application of external forces, which limits their applications [8].

Sludge is rich in hydrophilic functional groups, such as -OH and -COOH, that can form a stable and elastic network structure through adsorption bridging and act as a hydrogel-forming agent [9]. MS is mainly composed of C, O, N, S, P, and other elements. Among the components, carbon sources, including extracellular polymers, soluble sugars, cellulose, protein, and fats, account for about 50~80% of the total organic content in sludge [10,11]. Preliminary explorations into the feasibility of cracking and releasing organics from sludge have been performed in recent years [12–14]. Among these studies, solid CaO_2 to sludge was shown to dissolve in water to generate H_2O_2 at a controllable rate which in turn strongly oxidized the organic compounds to release them from the sludge [15]. However, the particle sizes in commercial CaO_2 are generally large, and as a result, the CaO_2 is not easy to disperse in the medium and tends to agglomerate, which reduces the surface contact area and reaction speed of CaO_2 and sludge flocs. The breakdown of the organics in sludge by CaO_2 is also limited, which requires the use of extra reagents to maintain good reactivity. In this paper, spherical nano-CaO_2 was synthesised and used as an activator for sludge and had a controllable reaction, high oxidation efficiency, better dispersion, and more significantly degraded the organic components of sludge compared with traditional commercial CaO_2 [16].

Extensive studies have investigated ways to utilize the organic carbon components in MS. Hossain et al. [17] used the carbon components from sludge to prepare biochar that was used to adsorb heavy metals in agricultural applications. Qin et al. [18] prepared a non-metallic electrocatalyst with excellent performance using MS as a raw material. Wang et al. [19] treated sludge with $FeCl_3$ and polyacrylamide and successfully prepared a carbon catalyst that had a mesoporous structure and multi-functional catalytic activity. Liang et al. [20] prepared a new type of activated carbon by co-pyrolysis of coconut shells and MS and found that its adsorption performance was far superior to other carbon adsorbents. The above studies highlight the feasibility of realizing high value-added products from the carbon components in sludge and also provide an experimental basis for the preparation of hydrogels from the carbon components released from sludge.

In this study, MS was used as a raw material, and synthesised nano-CaO_2 was used as an oxidant to stimulate the release of carbon components from sludge. Hydrogels were formed with added monomer (Acrylic acid, AA), a crosslinking agent (N,N′-methylenebisacrylamide, MBA) and an initiator (Ammonium persulfate, APS), and the remaining inorganic components in the sludge, such as SiO_2, Al_2O_3, and CaO, after the release of carbon-containing compounds dissolved as a rigid skeleton [21]. These inorganic-organic double network hydrogels were prepared by grafting copolymerisation. The effects of different preparation conditions on the swelling properties of the hydrogels are discussed. To

further optimise the synthetic methods, a comprehensive in-depth investigation on the related mechanisms is needed. Therefore, in this study, the interactions between the different preparation conditions on the resulting hydrogel properties were analysed using the response surface methodology (RSM). On this basis, the hydrogels were characterized by X-Ray diffraction (XRD), Scanning electron microscopy (SEM), and Fourier transform infrared spectroscopy (FT-IR), and the swelling mechanism of the hydrogels was analysed. These results are expected to provide a new approach for the high value-added utilization of MS.

2 Experimental Methods

2.1 Chemicals and Materials

The MS used in the experiments was obtained from a sewage-treatment plant in Xinzheng City of Zhengzhou (China) and was the primary dewatering sludge obtained from belt pressure filtration. The sludge was retrieved from the sewage treatment plant in batches and stored at 4°C. The service cycle of each batch of sludge was 7 d. After the time was exceeded, new sludge was collected, and its basic properties were determined. The organics content in the sludge samples ranged from 63.54%~68.88%, the water contents ranged from 83.26%~87.68%, and the pH values ranged from 7.20~7.64. AA, MBA, APS, and NaOH were all analytically pure and produced by Beijing InnoChem Technology Co., Ltd., Beijing, China.

The nano-CaO_2 used in the preparation of the hydrogels was first synthesised here. The particle sizes ranged from 45~300 nm, and the purity was 79.13%. XRD patterns and SEM images of the synthesised nano-CaO_2 are shown in Figs. 1 and 2. The mineral phases in traditional commercial CaO_2 and nano-CaO_2 synthesised here were the same. Both samples show XRD reflections at 2θ = 30.273°, 35.598°, 47.306° and 51.594° which were consistent with the characteristic peaks of CaO_2. However, some calcium hydroxide was also present in the commercially available calcium peroxide. As shown in Figs. 2a and 2b, it can be seen that there were obvious differences in the morphologies of the commercial CaO_2 and synthesised CaO_2. The commercial CaO_2 contained hexagonal particles and some irregularly shaped agglomerates. In contrast, the synthesised nano-CaO_2 were spherical or elliptical in shapes with particle sizes between 45 and 300 nm.

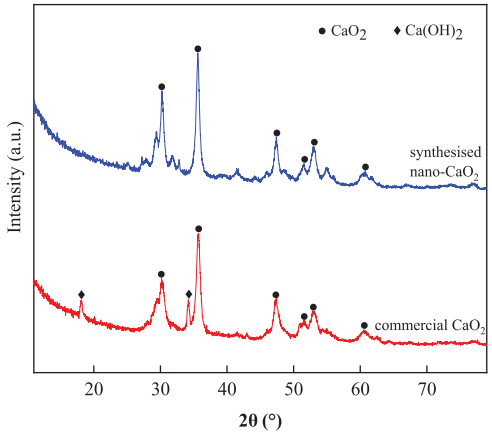

Figure 1: XRD patterns of commercial CaO_2 and synthesised nano-CaO_2

2.2 Principles and Processes for the Hydrogel Preparation

The hydrogel preparation protocol is shown schematically in Fig. 3. The hydrogel preparation mainly relied on crosslinking chemistries and free radical polymerisation as follows. The oxidation of CaO_2 was used to crack and release the carbon components (-OH, -COOH) in MS, and the decomposition of the organic matter resulted in the simultaneous release of the inorganic components (SiO_2, Al_2O_3, CaO).

Then, APS was used as an initiator that thermally decomposed at high temperature conditions to generate free radicals that extracted hydrogen atoms from the -OH groups in the main chain of organic components, which in turn formed active-OR. The added AA monomer was then initiated by the reactive radicals, and the C=C double bonds were opened and grafted onto the main chain of the organic components to form graft copolymers. The inorganic components, such as SiO_2, acted as cross-linking points between the layers of the hydrogel chains [22] and formed the first layer of the rigid inorganic network structure. The MBA acted as a cross-linking agent to promote crosslinking of branched chains to form a second layer of the flexible mesh structure of the hydrogel. Multiple components in the reaction mixture copolymerised resulting in interpenetration of the inorganic and organic networks to form the final inorganic-organic double network hydrogel.

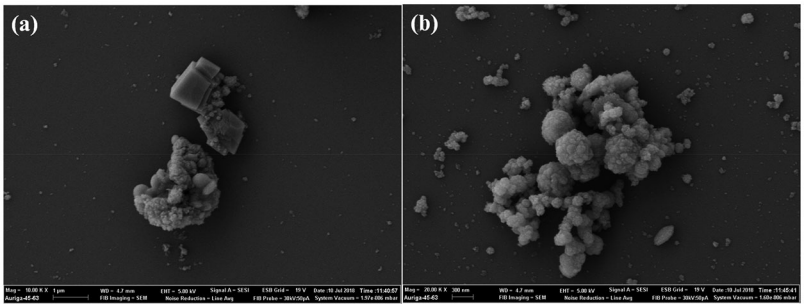

Figure 2: SEM images of (a) commercial CaO_2 and (b) synthesised nano-CaO_2

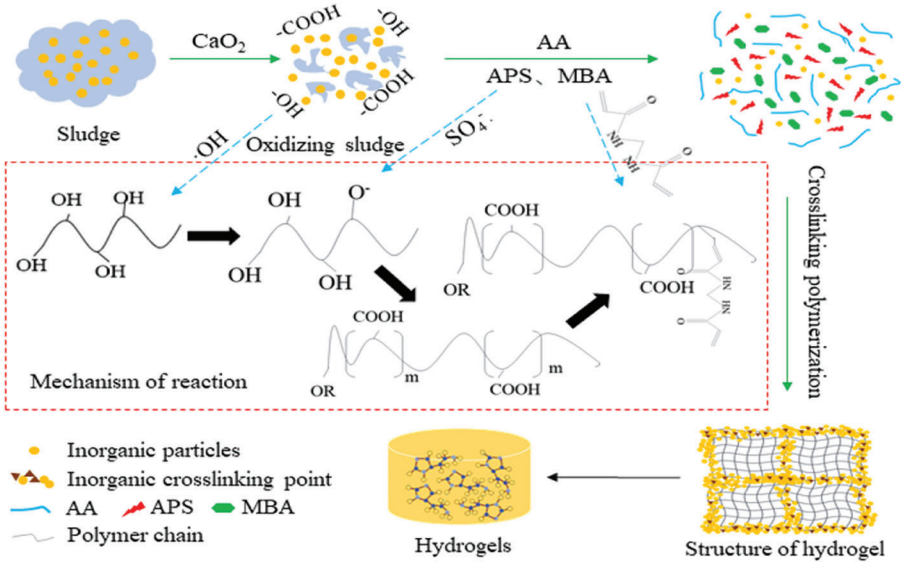

Figure 3: Schematic diagram of the hydrogel preparation process

A typical hydrogel preparation process was as follows. The desired amounts of sludge and deionized water at a mass ratio of 1:50 were weighed and mixed well to obtain a municipal sludge slurry (MSS). Then, 50 mL of MSS was added to a beaker, and CaO_2 was added. The mixture was placed in a constant temperature water bath and magnetically stirred (HSJ, Jiangsu Kexi Instrument Co., Ltd., Changzhou, China). The AA was added to the mixture after 30 min, and then an NaOH solution (5 mol/L) was added after 5 min to neutralise the AA. After 10 min of reaction, APS was added followed by MBA after an

additional 5 min. The water bath was maintained at a constant temperature, and the reaction mixture was stirred until a brown hydrogel formed. The solid hydrogel was the prepared municipal sludge hydrogel (MS-Hydrogel).

2.3 Determination of the Hydrogel Swelling Ratio

The prepared MS-Hydrogels were completely dried in a vacuum freeze dryer (LGJ-10, Beijing Yuechengjiaye Technology Co., Ltd., Beijing, China), and a certain mass of dry hydrogel was weighed. After the weight was recorded, the dry MS-Hydrogels were put into a beaker containing deionized water, and the beaker was placed in a constant temperature and humidity controlled artificial climate chamber (BIC-300, Shanghai Boxun Industrial Co., Ltd., Shanghai, China). The hydrogel was removed from the water every 2 h. After wiping the water off the surface of the hydrogel with absorbent paper, the hydrogel was weighed and then placed back in the beaker of water. The above process was repeated for a total of 12 h. The swelling ratio of MS-Hydrogel was calculated as shown in Eq. (1).

$$S_r = \frac{W_s - W_0}{W_0} \times 100\% \tag{1}$$

where S_r (%) is the swelling ratio of MS-Hydrogel, W_s (g) is the mass of MS-Hydrogel after swelling and water absorption, W_0 (g) is the mass of MS-Hydrogel before swelling.

Fig. 4 presents images of the prepared MS-Hydrogel, Freeze-dried MS-Hydrogel, and MS-Hydrogel after 12 h of water absorption.

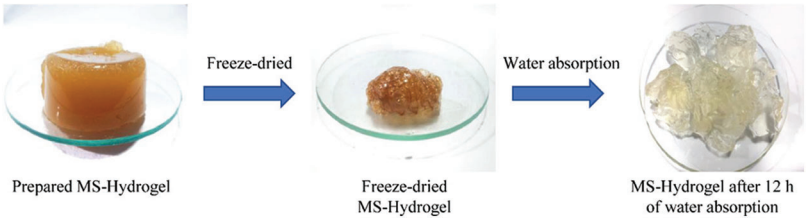

Figure 4: Photographs of different forms of the MS-Hydrogels

2.4 RSM Experimental Design

The Box-Behnken experimental design was chosen to evaluate the combined effects of four independent variables that were identified to affect the hydrogel swelling properties using single factor tests at three levels as shown in Table 1. All the experiments were conducted in triplicate, and the average of the S_r value was taken as response. The experimental data were analysed with the RSM procedure and fitted to an empirical quadratic model.

Table 1: Factors and levels of the MS-Hydrogel swelling ratio

Levels	Factors			
	nano-CaO_2 (g): A	AA (g): B	APS (g): C	MBA (g): D
−1	0.15	5.6	0.10	0.10
0	0.20	5.8	0.15	0.15
1	0.25	6.0	0.20	0.20

2.5 Characterisation of the Hydrogel Properties

The surface chemical composition of the hydrogels was determined using X-ray Photoelectron Spectroscopy (D8 ADVANCE, Bruker Corporation, Milton, ON, Canada). The functional groups present in the MS and MS-Hydrogels were measured by FTIR spectroscopy (Nicolet 6700, Thermo Fisher Scientific, Waltham, MA, USA) using the KBr pellet technique and were examined in the 4000~500/cm region. The morphologies of the MS and MS-Hydrogel were characterized by SEM (Quanta 250, FEI, Ltd., Brno, Czech Republic).

3 Results and Analysis

3.1 Effect of Preparation Conditions on the Swelling Properties of the Hydrogels

3.1.1 Effect of Polymerisation Temperature on the MS-Hydrogel Swelling Ratio

To investigate the effects of the polymerisation temperature on the hydrogel properties, the polymerisation was performed with the volume of MSS held constant at 50 mL, the CaO_2 dosage controlled to 0.15 g, a constant AA dosage of 5.6 g and AA neutralisation of 60%, a fixed APS dosage of 0.20 g and a fixed MBA dosage of 0.10 g. The effects of the polymerisation temperature on the swelling ratio are shown in Fig. 5.

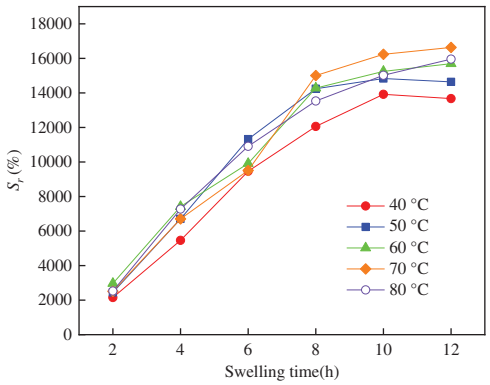

Figure 5: Effect of polymerisation temperature on the swelling ratio of the hydrogels

As seen in, Fig. 5, the S_r of the MS-Hydrogels prepared at all temperature increased over time. Comparing the S_r at 12 h suggested that the swelling ratio first increased and then decreased with increasing polymerisation temperature. When the polymerization temperature was 70°C, S_r reached a maximum value of 16636.9%. This was due to the low rate of APS decomposition and slower free radical polymerisation kinetics at low temperatures. Due to the lower degrees of cross-linking at these conditions [23], the networks formed were "defective" and incomplete, and the water-holding capacity of the MS-Hydrogels was poor. The decomposition of APS accelerated at higher polymerisation temperatures, and the probability of collisions between the different components and free radicals in the system increased, which promoted the formation of the hydrogel network structure. As a result, S_r gradually increased with reaction temperature. However, when the temperature was too high, the APS decomposed rapidly and reacted violently, and the polymerization reaction was too fast. At high temperatures, the extent of reaction was too high in some areas and not high enough in other areas, which prevented the formation of a uniform and effective network structure and led to the decrease in the hydrogel swelling performance.

3.1.2 Effect of Degree of Monomer Neutralisation on the MS-Hydrogel Swelling Ratio

The effects of the degree of monomer neutralisation on the hydrogel swelling ratio are shown in Fig. 6. For these experiments, the other variables were kept constant including 50 mL of MSS, a controlled CaO_2 dosage of 0.15 g, an AA dosage of 5.6 g, an APS dosage of 0.20 g, an MBA dosage of 0.10 g, and a polymerization temperature of 70°C.

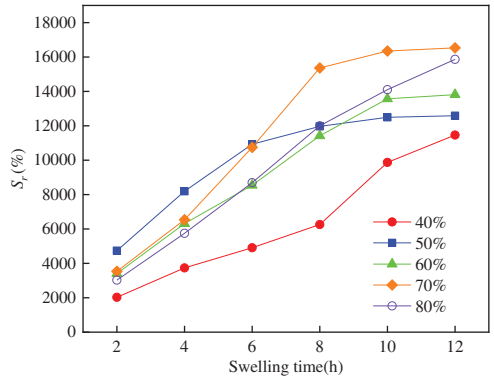

Figure 6: Effect of degree of monomer neutralisation on the swelling ratios of the hydrogels

As shown in Fig. 6, the S_r of MS-Hydrogel prepared under different extents of AA neutralisation increased with an increase in the swelling time, and the S_r first increased and then decreased as the degree of neutralisation increased. This trend was because when the degree of neutralisation of AA was lower than 70%, more -COOH groups were present in the system, and these groups tended to self-polymerise which increased the overall crosslinking density and decreased the water retention of the hydrogel [24]. A maximum S_r value of 16530.2% was measured for the hydrogel with a degree of neutralisation of 70%. When the degree of neutralization was higher than 70%, slow conversion of AA prevented the formation of well-defined network structure and decreased the absorbency of the hydrogel [25].

3.1.3 Effect of CaO_2 Dosage on the MS-Hydrogels Swelling Ratio

These experiments used 50 mL of MSS, controlled the amount of AA to 5.6 g, fixed the degree of AA neutralisation to 70%, used 0.20 g of APS and 0.10 g of MBA, and fixed the polymerization temperature at 70°C. The effects of CaO_2 dosage on the MS-Hydrogel swelling properties at these conditions are presented in Fig. 7.

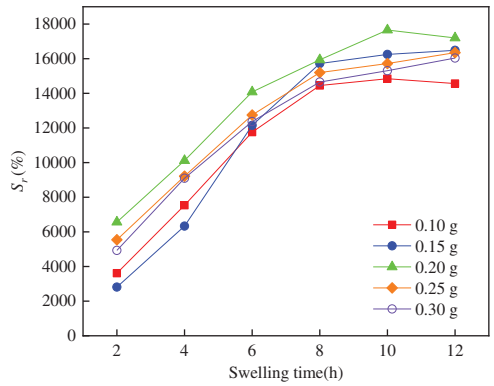

Figure 7: Effect of CaO_2 dosage on the swelling ratios of the hydrogels

As seen in Fig. 7, S_r increased with CaO_2 dosage for hydrogels prepared with less than 0.2 g of CaO_2. At these dosages, CaO_2 generated $Ca(OH)_2$ and H_2O_2 in the liquid system [26], and the metal ions present in low concentrations in MS acted as catalysts to convert H_2O_2 to ·OH. As a result, the H_2O_2 generated was less stable. Moreover, the thermal activation of APS at the high temperatures formed SO_4^{-}·, which is also a strong oxidizer. The alkalinity of $Ca(OH)_2$ and the oxidation of ·OH and SO_4^{-}· promoted degradation of the organic components in the sludge and release of the carbon components.

When the dosage of CaO_2 was 0.20 g, S_r reached a maximum of 17197.0%. At even higher CaO_2 dosages, the S_r decreased as the CaO_2 dosages continued to increase. At high dosages, the added Ca^{2+} led to flocculation of the components in the sludge [27], thus hindering the formation of the hydrogel network. Moreover, high concentrations of Ca^{2+} in the system also formed salt bridges with the polysaccharide molecules, which ordered the molecules and increased the number of entanglements [28], and both of these effects led to a decrease in the swelling properties of the hydrogels.

3.1.4 Effect of Initiator Dosage on the MS-Hydrogel Swelling Ratio

To study the effects of initiator dosage on the MS-Hydrogel properties, all other reaction conditions were held constant at 50 mL of MSS, 0.20 g of CaO_2, 5.6 g of AA, a degree of neutralisation of 70%, an MBA dosage of 0.10 g, and a polymerisation temperature of 70°C, the results are shown in Fig. 8.

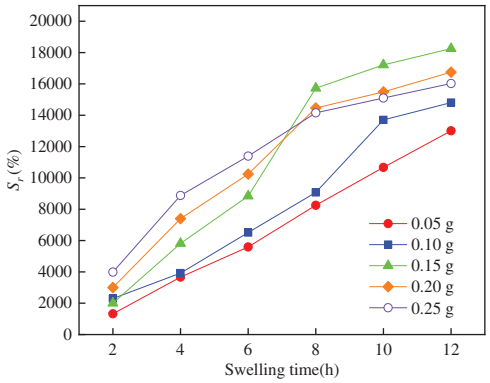

Figure 8: Effect of initiator dosage on the swelling ratio of the MS-Hydrogels

As shown in Fig. 8, after 12 h of swelling, S_r first increased and then decreased with increasing of APS dosage. The maximum S_r value of 18252.0% was measured for the hydrogel prepared with 0.15 g of APS. The reactions involving APS are shown in Eqs. (2) to (4).

$$(NH_4)_2S_2O_8 \rightleftharpoons 2NH_4^{+} + S_2O_8^{2-} \tag{2}$$

$$(NH_4)_2S_2O_8 + H_2O \rightleftharpoons 2NH_4HSO_4 + H_2O_2 \tag{3}$$

$$S_2O_8^{2-} + 2H_2O \rightleftharpoons 2HSO_4^{-} + H_2O_2 \tag{4}$$

In this process, the APS was thermally activated to produce SO_4^{-}· as shown in Eq. (5) [29].

$$^{\ominus}O-\overset{\overset{O}{\|}}{\underset{\underset{O}{\|}}{S}}-O-O-\overset{\overset{O}{\|}}{\underset{\underset{O}{\|}}{S}}-O^{\ominus} \xrightarrow{heat} 2(\cdot OSO_2O^{\ominus}) \tag{5}$$

In the initial stage of the reaction, as the APS dosage increased, the associated increase in the free radical concentration polymerised the AA and carbon sources in the sludge to form a three-dimensional network structure. At too high of dosages, the copolymerization and self-polymerization reactions were too fast

which decreased the relative molecular weight of the formed polymers, shortened the hydrogel backbone length and led to a decrease in the swelling properties of the hydrogels [30].

3.1.5 Effects of Monomer Dosage on the MS-Hydrogels Swelling Ratio

The MSS volume was constant at 50 mL, the CaO_2 dosage was 0.20 g, the degree of neutralisation was 70%, the APS amount was 0.15 g, the amount of MBA was 0.10 g, and the polymerization temperature was 70°C to investigate the effects AA dosage on the properties of the MS-Hydrogels. The results are shown in Fig. 9.

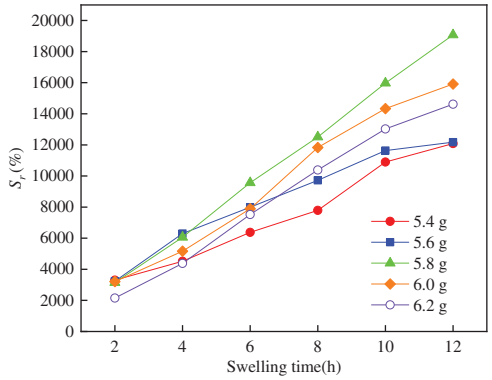

Figure 9: Effect of monomer dosage on the swelling ratio of the MS-Hydrogels

The S_r increased and then decreased with increasing amounts of AA. The maximum S_r of 19072.7% was measured for the hydrogel prepared with 5.8 g of AA. The increase at low AA dosages was due to the fact that AA molecules could self-polymerise or graft copolymerise with the carbon components in the sludge, and the AA molecules contained a large number of hydrophilic -COOH groups which allowed the hydrogel to absorb a large amount of water without dissolving [31]. At AA amounts greater than 5.8 g, the S_r decreased, because the degree of crosslinking increased. At high crosslinking densities, the polymer chain motions in the hydrogel were restricted, the network wall thickness increased, the pore sizes became smaller [32], and the ductility of the hydrogel was limited, which decreased the swelling performance.

3.1.6 Effect of Crosslinking Agent Dosage on the MS-Hydrogels Swelling Ratio

The amount of MBA added to the hydrogel was varied at a constant MSS volume of 50 mL MSS, a controlled CaO_2 dosage of 0.20 g, a fixed AA dosage of 5.8 g, a constant AA degree of neutralisation of 70%, a fixed APS dosage of 0.15 g, and a polymerisation temperature of 70°C. The swelling ratios of the resulting hydrogels are shown in Fig. 10.

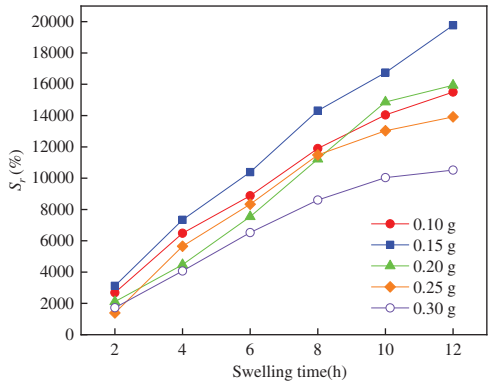

Figure 10: Effect of crosslinking agent dosage on the swelling ratios of the MS-Hydrogels

As shown in Fig. 10, with an increase in the amount of MBA added, the S_r of the hydrogels first increased and then decreased. A maximum S_r of 19768.4% was measured for the hydrogel prepared with 0.15 g of MBA. This nonmonotonic trend was because up to a certain point, the increased MBA dosage increased the crosslinking density which improved the water-holding performance of the hydrogels [33]. When too much MBA was added, the MBA self-polymerised which increased the crosslinking density and decreased the porosity of the hydrogel which decreased the swelling performance [34].

3.2 RSM Analysis

In order to determine the optimal reaction conditions to prepare an MS-Hydrogel with the highest S_r and to determine whether there were interactions between the different reaction conditions on the properties of the resulting hydrogels, a multiple second-order polynomial equation was fit to the experimental data as shown in Eq. (6).

$$Y = 19367.64 - 814.72 \times A + 224.05 \times B + 281.74 \times C - 1053.88 \times D + 29.30 \times AB - 491.45 \times AC + 1016.00 \times AD + 884.84 \times BC - 812.22 \times BD - 694.80 \times CD - 3263.07 \times A^2 - 2791.60 \times B^2 - 4332.86 \times C^2 - 1658.76 \times D^2 \quad (6)$$

where A, B, C, D and Y are the dosage of nano-CaO_2, monomer, initiator, cross-linking agent and S_r, respectively. The Model F-value from the variance analysis for the response surface quadratic model was 14.75 which implied that the model was significant, and there was only a 0.01% chance that a "Model F-value" this large was due to noise. Values of "Prob > F" were less than 0.0500 which indicated that the model terms were significant. The F-value of 3.60 implied that the "Lack of Fit" was not significant relative to the error, which was good for the model. The adequacy and the significance of the response surface model were determined based on an analysis of the variance. The analysis showed that the squared regression statistic (R^2) was 0.9365, and the difference between the "Adj R-Squared" and "Pred R-Squared" was 0.2100, which indicated a good consistency between the experimental and predicted values and implied that the mathematical model was reliable. The value of the C.V.% (coefficient of variation), 7.01%, also suggested that the model was highly accurate and reproducible. The actual and predicted experimental values were linear as shown in Fig. 11, indicating that these values were well correlated.

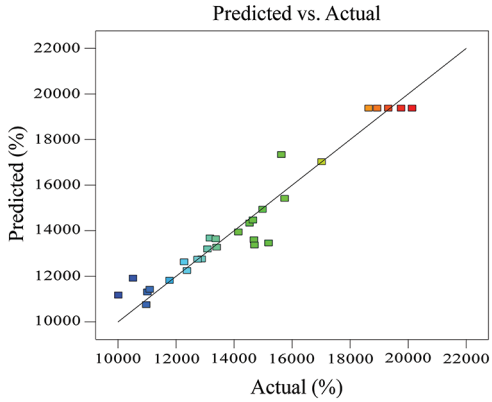

Figure 11: Comparison of predicted and measured results

Fig. 12 presents the three-dimensional response surfaces and their corresponding two-dimensional circular contour plots generated by the Design Expert Software Package. The response surface plots showed that AB, AC, AD, BC, BD, and CD had interacting effects on S_r. For optimization, all input variables were kept 'in range', and S_r was maximized in numerical the optimization section of software.

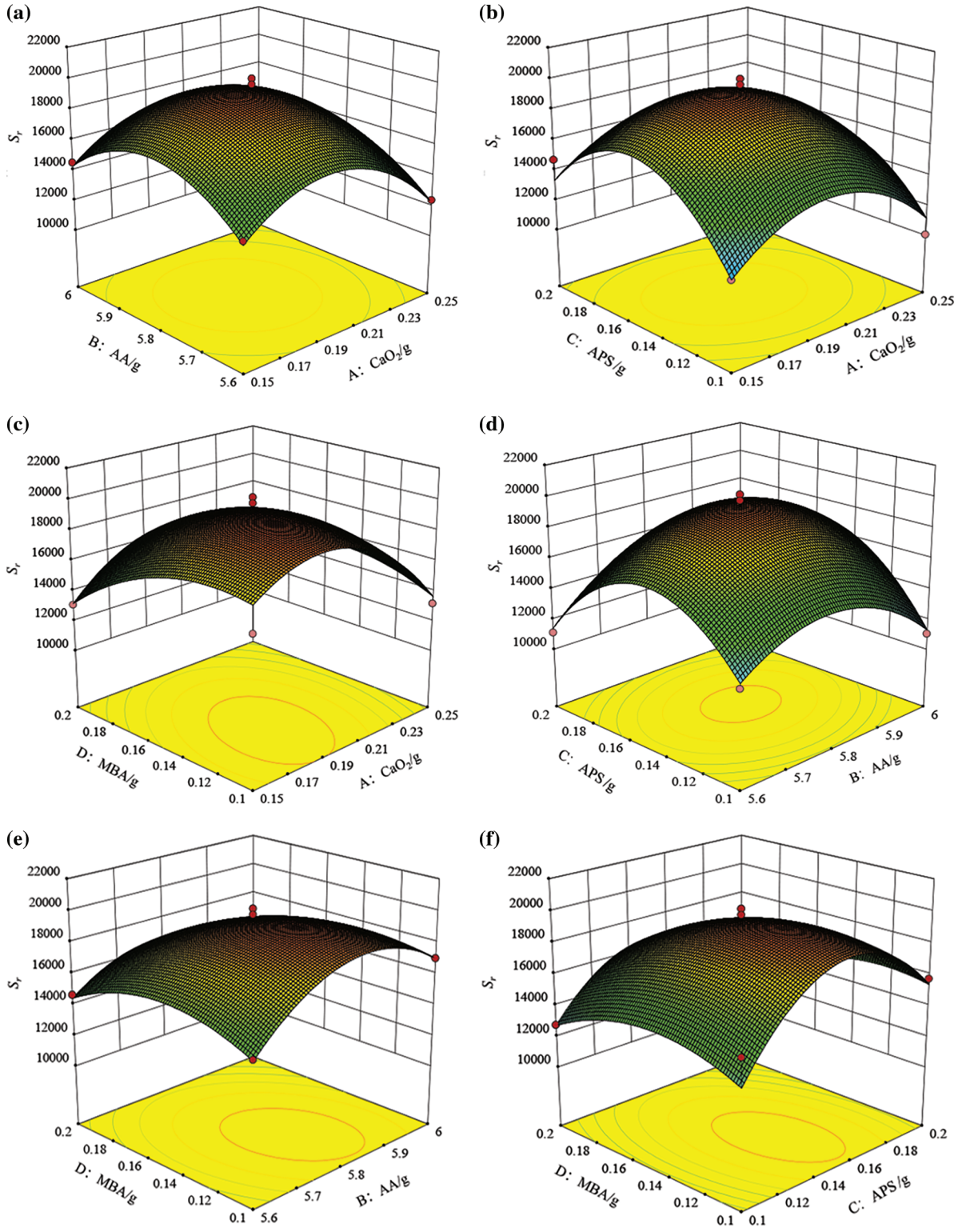

Figure 12: Response surface plots of CaO_2 dosage *vs.* AA dosage; (b) CaO_2 dosage *vs.* APS dosage; (c) CaO_2 dosage *vs.* MBA dosage; (d) AA dosage *vs.* APS dosage; (e) AA dosage *vs.* MBA dosage; (f) APS dosage *vs.* MBA dosage

The optimum values were 0.190 g, 5.823 g, 0.155 g, and 0.129 g for A, B, C, and D, respectively, for attaining a hydrogel with a maximum S_r (i.e., 19697.883%).

Three additional experiments using each optimum operating condition determined from the RSM model were conducted to validate the model. The process variable solutions and experimental results are listed in Table 2. The replicate experiments yielded MS-Hydrogel with an S_r of 14837.2%, 14042.6%, and 13386.1%, respectively. The results clearly demonstrate the effectiveness of the model to optimize the composite conditioning effects.

Table 2: Verification experiments at predicted optimum conditions

CaO_2/g	AA/g	APS/g	MBA/g	S_r/%	
				Predicted value	Actual value
0.15	5.6	0.15	0.15	14159.6	14837.2
0.25	5.8	0.15	0.10	13180.7	14042.6
0.20	5.6	0.15	0.20	14663.0	13386.1

3.3 Phase, Morphology, and Structural Analysis of the MS-Hydrogels

3.3.1 XRD Characterization Results

The MS-Hydrogel prepared at the optimal reaction conditions sample was dried, ground into a powder, passed through a 300 mesh sieve, coated and then measured with XRD. XRD measurements were performed with a Cu Kα source at a current of 30 mA and a voltage of 35 kV, and the scanning range was 2θ = 15°–75°. The XRD spectra are shown in Fig. 13.

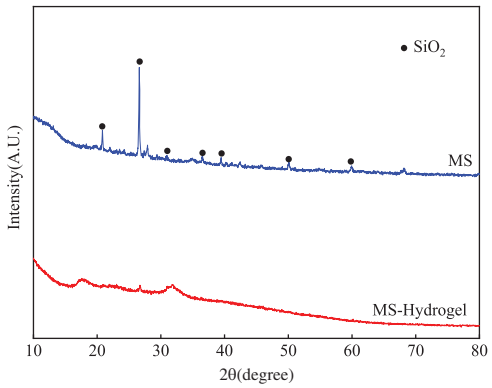

Figure 13: XRD patterns of MS and the MS-Hydrogel

Sharp diffraction peaks were seen in the pattern measured of MS at 2θ = 20.84°, 26.61°, 30.89°, 36.50°, 39.44°, 50.12° and 59.91°, which corresponded to the diffraction peaks typically measured for crystalline SiO_2 [35]. The intensity of the diffraction peaks at scattering angles greater than 2θ = 30° was relatively low and suggested a large amount of amorphous CH material was also present in the sludge. The diffraction patterns of the MS-Hydrogel showed two broad peaks, one between 2θ = 15°–20°, and the other between 2θ = 30°–35°, indicating that structure was amorphous. A low intensity at 2θ = 26.61° was still present which corresponded to (101) crystalline plane of SiO_2, indicating that the crystallinity of SiO_2 was reduced during the cross-linking polymerisation reaction, the intermolecular hydrogen bonds were broken, and the crystal shape changed.

3.3.2 SEM Characterization Results

The structures of the MS, freeze-dried MS-Hydrogel, brittle fractured MS-Hydrogel, and swelling MS-Hydrogel sample were imaged with SEM. The samples were sprayed with gold before being imaged, and the results are shown Fig. 14.

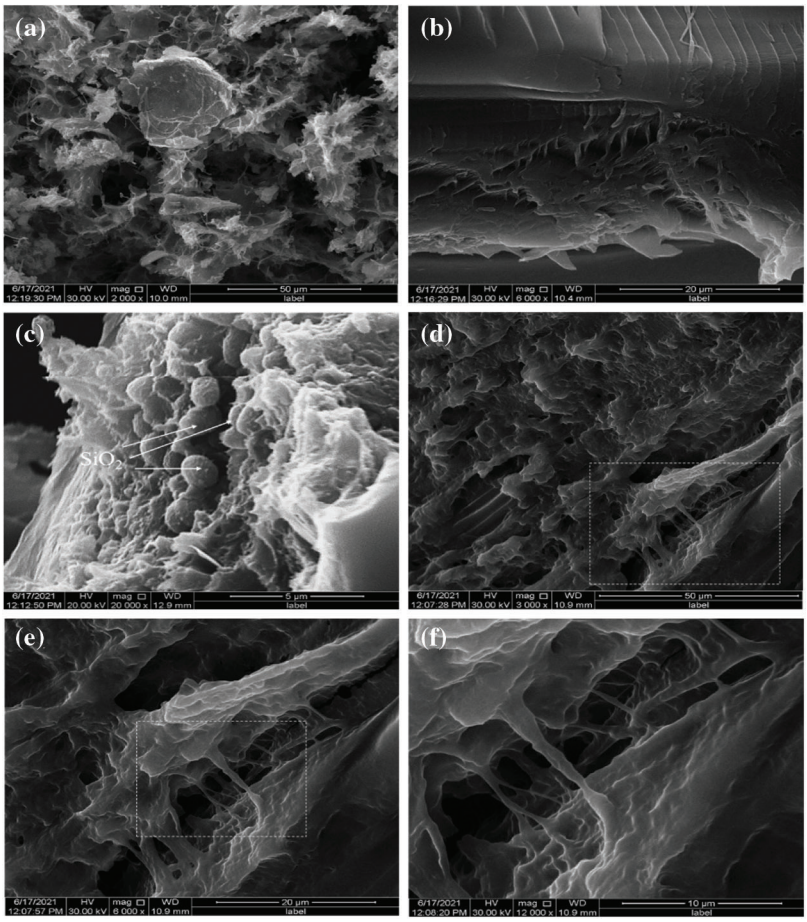

Figure 14: SEM images of the MS sludge and MS-Hydrogels. (a) MS; (b) Freeze-dried MS-Hydrogel; (c) Brittle fracture of MS-Hydrogel; (d) Swollen MS-Hydrogel × 3000; (e) Swollen MS-Hydrogel × 6000; (f) Swollen MS-Hydrogel × 12000

A typical fractal floc structure similar to a branching broken fluff structure was seen in the MS in Fig. 14a [36]. Meanwhile, as shown in Fig. 14b, the structure of the freeze-dried MS-Hydrogel showed irregular interlaced folds with thick pore walls and indistinct pores, suggesting that the local network structure had contracted. In Fig. 14c, spherical SiO_2 particles embedded in a mesh-like structure were seen in the cross-section of the fractured MS-Hydrogel, which suggested that the SiO_2 particles acted as cross-linking points to form an inorganic-organic double network. As described in previous studies of gels, the SiO_2 particles penetrated through the layers of MS-Hydrogel chains which formed pores [37] and increased the contact area between the MS-Hydrogel and H_2O to improve the swelling performance of the hydrogel [38]. As seen in Fig. 14d through Fig. 14f, the three-dimensional network in the MS-Hydrogel swelled and pores were visible as water molecules entered the structure [39].

3.3.3 FT-IR Characterization Results

The MS and MS-Hydrogel were characterized with FT-IR. The results are shown in Fig. 15.

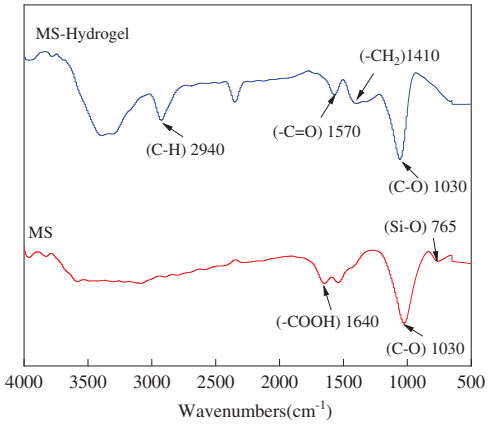

Figure 15: FT-IR analysis of MS and MS-Hydrogel

As can be seen from Fig. 15, there were three distinct absorption peaks in the spectrum of the MS at wavelengths of 765, 1030 and 1640 cm^{-1}, corresponding to the infrared absorption peaks of Si-O bonds in SiO_2 and C-O and -COOH groups in the organic matter, respectively [40]. Meanwhile, the broad peaks between 3300 to 3500 cm^{-1} in the spectrum of the MS-Hydrogel were due to the presence of the $-NH_2$ and -NH groups [41]. The absorption peak at 2940 cm^{-1} was assigned as the anti-symmetric stretching peak of C-H, and the absorption peak -C=O at 1570 cm^{-1} was due to the interactions between the amide groups in MBA and -C=O groups in acrylic acid. Peaks corresponding to the bending vibrations of C-H in $-CH_2$ appeared at 1410 cm^{-1} [42], from which it could be speculated that the MBA in the MS-Hydrogel was grafted onto the carbon skeleton in the MS, and the grafting polymerisation reaction occurred between the introduced MBA and AA and the carbon components in the sludge. It can also be speculated that the oxygen-containing functional groups, such as -COOH and C=O, participated in the MS-Hydrogel formation through surface complexation reactions.

4 Conclusions

(a) Synthesised nano-CaO_2 was used as an oxidant to stimulate the release of carbon sources in MS, and the optimum process parameters for preparing the hydrogels were determined through single factor experiments to be a dosage of CaO_2 of 0.20 g, an AA dosage of 5.8 g, an AA neutralisation degree of 70%, an APS dosage of 0.15 g, an MBA dosage of 0.15 g, a polymerization temperature of 70°C. The swelling ratios of hydrogels prepared with these conditions reached 19768.4% at 12 h.

(b) The hydrogel preparation conditions were optimized using the response surface method, and the interactions between the different factors were analysed. It was found that the relative error of the predicted hydrogel swelling ratio in the regression model was less than 5% compared with the actual experimental value, and the model could be used to predict the experimental results.

(c) XRD characterization results showed that while the inorganic components in the MS sludge were highly crystalline, the MS-Hydrogel was primarily amorphous. During the crosslinking polymerisation reaction, the crystallinity in the sludge was reduced and the intermolecular hydrogen bonds were destroyed, resulting in a change in the crystal shape.

(d) SEM characterization results indicated that the SiO_2 in the sludge acted as cross-linking points in the hydrogels that connected the hydrogel chains, thus forming more pores. The hydrogel structure was

highly stretched after swelling, and the dual inorganic-organic network structure and high flexibility of the prepared hydrogels were the main reasons for their high swelling properties.

(e) FT-IR analysis indicated that oxygen-containing functional groups, such as -COOH and C=O, in the carbon-containing compounds from the sludge participated in the hydrogel synthesis through surface complexation reactions.

Funding Statement: The authors acknowledge the support from the National Visiting Scholar Program for Key Young Teachers of Central and Western Universities, the Ministry of Education (19042), the Key Science and Technology Project of Henan Province (212102310064), the National Innovation and the Entrepreneurship Training Program for College Students, Ministry of Education (202111517002).

Conflicts of Interest: The authors declare that they have no conflicts of interest to report regarding the present study.

References

1. Zhang, S., Wang, F., Mei, Z. Y., Lv, L., Chi, Y. (2020). Status and development of sludge incineration in China. *Waste and Biomass Valorization, 12(7),* 3541–3574. DOI 10.1007/s12649-020-01217-9.
2. Lu, J. Y., Wang, X. M., Liu, H. Q., Yu, H. Q., Li, W. W. (2019). Optimizing operation of municipal wastewater treatment plants in China: The remaining barriers and future implications. *Environment International, 129,* 273–278. DOI 10.1016/j.envint.2019.05.057.
3. Wei, L. L., Zhu, F. Y., Li, Q. Y., Xue, C. H., Xia, X. et al. (2020). Development, current state and future trends of sludge management in China: Based on exploratory data and CO_2-equivaient emissions analysis. *Environment International, 144(3),* 106093. DOI 10.1016/j.envint.2020.106093.
4. Pourjavadi, A., Tehrani, Z. M., Salami, H., Seidi, F., Motamedi, A. et al. (2020). Both tough and soft double network hydrogel nanocomposite based on o-carboxymethyl chitosan/poly (vinyl alcohol) and graphene oxide: A promising alternative for tissue engineering. *Polymer Engineering & Science, 60(5),* 889–899. DOI 10.1002/pen.25297.
5. Cheng, D., Liu, Y., Yang, G., Zhang, A. (2018). Water- and fertilizer-integrated hydrogel derived from the polymerization of acrylic acid and urea as a slow-release N fertilizer and water retention in agriculture. *Journal of Agricultural and Food Chemistry, 66(23),* 5762–5769. DOI 10.1021/acs.jafc.8b00872.
6. Peng, X. W., Zhong, L. X., Ren, J. L., Sun, R. C. (2012). Highly effective adsorption of heavy metal ions from aqueous solutions by macroporous xylan-rich hemicelluloses-based hydrogel. *Journal of Agricultural and Food Chemistry, 60(15),* 3909–3916. DOI 10.1021/jf300387q.
7. Womack, N. C., Piccoli, I., Camarotto, C., Squartini, A., Guerrini, G. (2022). Hydrogel application for improving soil pore network in agroecosystems. Preliminary results on three different soils. *Catena, 208,* 105759. DOI 10.1016/j.catena.2021.105759.
8. Zhao, F. L., Yao, D., Guo, R. W., Deng, L. D., Dong, A. J. et al. (2015). Composites of polymer hydrogel and nanoparticulate systems for biomedical and pharmaceutical applications. *Nanomaterials, 5(4),* 2054–2130. DOI 10.3390/nano5042054.
9. Seviour, T., Pijuan, M., Nicholson, T., Keller, J., Yuan, Z. G. (2009). Gel-forming exopolysaccharides explain basic differences between structures of aerobic sludge granules and floccular sludges. *Water Research, 43(18),* 4469–4478. DOI 10.1016/j.watres.2009.07.018.
10. Wei, S. Z., Xiao, B. Y., Liu, J. X. (2010). Impact of alkali and heat pretreatment on the pathway of hydrogen production from sewage sludge. *Chinese Science Bulletin, 55(8),* 777–786. DOI 10.1007/s11434-009-0591-7.
11. Tang, Y. F., Dai, X. H., Dong, B., Guo, Y. Q., Dai, L. L. (2020). Humification in extracellular polymeric substances (EPS) dominates methane release and EPS reconstruction during the sludge stabilization of high-solid anaerobic digestion. *Water Research, 175(2),* 115686. DOI 10.1016/j.watres.2020.115686.
12. Zhang, A., Wang, J., Li, Y. M. (2015). Performance of calcium peroxide for removal of endocrine-disrupting compounds in waste activated sludge and promotion of sludge solubilization. *Water Research, 71(15),* 125–139. DOI 10.1016/j.watres.2015.01.005.

13. Chen, Z., Zhang, W. J., Wang, D. S., Ma, T., Bai, R. Y. et al. (2016). Enhancement of waste activated sludge dewaterability using calcium peroxide pre-oxidation and chemical re-flocculation. *Water Research, 103(15),* 170–181. DOI 10.1016/j.watres.2016.07.018.
14. Wu, B. R., Chai, X. L. (2016). Novel insights into enhanced dewatering of waste activated sludge based on the durable and efficacious radical generating. *Journal of the Air & Waste Management Association, 66(11),* 1151–1163. DOI 10.1080/10962247.2016.1189858.
15. Northup, A., Cassidy, D. (2008). Calcium peroxide (CaO_2) for use in modified Fenton chemistry. *Journal of Hazardous Materials, 152(3),* 1164–1170. DOI 10.1016/j.jhazmat.2007.07.096.
16. Li, Y. L., Liu, L., Li, K. P., Lin, K., Dou, X. et al. (2021). Preparation of spherical nano-CaO_2 and its application in sludge deep-dewatering coupled with electro-osmotic. *Chemical Industry and Engineering Progress, 40(7),* 4047–4054. DOI 10.16085/j.issn.1000-6613.2020-1552.
17. Hossain, M. K., Strezov, V., Chan, K. Y., Ziolkowski, A., Nelson, P. F. (2011). Influence of pyrolysis temperature on production and nutrient properties of wastewater sludge biochar. *Journal of Environmental Management, 92(1),* 223–228. DOI 10.1016/j.jenvman.2010.09.008.
18. Qin, Z. Y., Jiang, X. P., Cao, Y., Dong, S. S., Wang, F. et al. (2021). Nitrogen-doped porous carbon derived from digested sludge for electrochemical reduction of carbon dioxide to formate. *Science of the Total Environment, 759,* 143575. DOI 10.1016/j.scitotenv.2020.143575.
19. Wang, X. P., Gu, L., Zhou, P., Zhu, N. W., Li, C. X. et al. (2017). Pyrolytic temperature dependent conversion of sewage sludge to carbon catalyst and their performance in persulfate degradation of 2-Naphthol. *Chemical Engineering Journal, 324,* 203–215. DOI 10.1016/j.cej.2017.04.101.
20. Liang, Q. L., Liu, Y. C., Chen, M. Y., Ma, L. L., Yang, B. et al. (2020). Optimized preparation of activated carbon from coconut shell and municipal sludge. *Materials Chemistry and Physics, 241(3),* 122327. DOI 10.1016/j.matchemphys.2019.122327.
21. Zhou, Y. F., Li, J. S., Lu, J. X., Cheeseman, C., Poon, C. S. (2020). Sewage sludge ash: A comparative evaluation with fly ash for potential use as lime-pozzolan binders. *Construction and Building Materials, 242(5),* 118160. DOI 10.1016/j.conbuildmat.2020.118160.
22. Donatello, S., Tyrer, M., Cheeseman, C. R. (2010). Eu landfill waste acceptance criteria and EU hazardous waste directive compliance testing of incinerated sewage sludge ash. *Waste Management, 30(1),* 63–71. DOI 10.1016/j.wasman.2009.09.028.
23. Jayaramudu, T., Ko, H. U., Kim, H. C., Kim, J. W., Kim, J. (2019). Swelling behavior of polyacrylamide-cellulose nanocrystal hydrogel: Swelling kinetics, temperature, and pH effects. *Materials, 12(13),* DOI 10.3390/ma121320802080.
24. Cheng, W. M., Hu, X. M., Wang, D. M., Liu, G. H. (2015). Preparation and characteristics of corn straw-Co-AMPS-Co-AA superabsorbent hydrogel. *Polymers, 7(11),* 2431–2445. DOI 10.3390/polym7111522.
25. Marandi, G. B., Mahdavinia, G. R., Ghafary, S. (2011). Collagen-g-poly (Sodium Acrylate-co-Acrylamide)/sodium montmorillonite superabsorbent nanocomposites: Synthesis and swelling behavior. *Journal of Polymer Research, 18(6),* 1487–1499. DOI 10.1007/s10965-010-9554-6.
26. Arienzo, M. (2000). Degradation of 2,4,6-trinitrotoluene in water and soil slurry utilizing a calcium peroxide compound. *Chemosphere, 40(4),* 331–337. DOI 10.1016/S0045-6535(99)00212-X.
27. Higgins, M. J., Novak, J. T. (1997). Dewatering and settling of activated sludges: The case for using cation analysis. *Water Environment Research, 69(2),* 225–232. DOI 10.2175/106143097X125380.
28. Yan, J. X., Zhang, B. Y., Wu, F. F., Yan, W. J., Lv, P. et al. (2020). Diverse mechanical properties and microstructures of sorghum bran arabinoxylans/soy protein isolate mixed gels by duo-induction of peroxidase and calcium ions. *Food Hydrocolloids, 107(4),* 105946. DOI 10.1016/j.foodhyd.2020.105946.
29. Tan, C. Q., Gao, N. Y., Deng, Y., An, N., Deng, J. (2012). Heat-activated persulfate oxidation of diuron in water. *Chemical Engineering Journal, 203(5),* 294–300. DOI 10.1016/j.cej.2012.07.005.
30. Wang, Y. Z., Shi, X. N., Wang, W. B. (2013). Synthesis, characterization, and swelling behaviors of a pH-responsive CMC-g-poly (AA-co-AMPS) superabsorbent hydrogel. *Turkish Journal of Chemistry, 37(1),* 149–159. DOI 10.3906/kim-1204-52.

31. Shi, X. N., Wang, W. B., Wang, A. Q. (2011). Effect of surfactant on porosity and swelling behaviors of guar gum-g-poly (sodium acrylate-co-styrene)/attapulgite superabsorbent hydrogel. *Colloids and Surfaces B: Biointerfaces, 88(1),* 279–286. DOI 10.1016/j.colsurfb.2011.07.002.
32. Pourjavadi, A., Barzegar, S., Mahdavinia, G. R. (2006). Mba-crosslinked Na-Alg/CMC as a smart full-polysaccharide superabsorbent hydrogel. *Carbohydrate Polymers, 66(3),* 386–395. DOI 10.1016/j.carbpol.2006.03.013.
33. Zhou, T., Wang, Y., Huang, S., Zhao, Y. C. (2018). Synthesis composite hydrogel from inorganic-organic hybrids based on leftover rice for environment-friendly controlled-release urea fertilizers. *Science of the Total Environment, 615,* 422–430. DOI 10.1016/j.scitotenv.2017.09.084.
34. Li, A., Wang, A. Q., Chen, J. M. (2010). Studies on poly (acrylic acid)/attapulgite superabsorbent composite. I. Synthesis and characterization. *Journal of Applied Polymer Science, 92(3),* 1596–1603. DOI 10.1002/app.20104.
35. Liu, J., Li, J. F., Luo, Z. P., Liu, Y. B., Liu, Z. X. et al. (2019). A novel multiwalled LiF@ GO@ SiO_2 microcapsule with high phase change temperature. *Solar Energy Materials and Solar Cells, 203,* 110188. DOI 10.1016/j.solmat.2019.110188.
36. Cândido, J. D. S., Leitão, R. C. F., Ricardo, N. M. P. S., Feitosa, J. P. A., Muniz, E. C. et al. (2012). Hydrogel composite of poly (acrylamide-co-acrylate) and rice husk ash. I. Synthesis and characterization. *Journal of Applied Polymer Science, 123(2),* 879–887. DOI 10.1002/app.34528.
37. Pan, Z. H., Huang, Y. R., Guo, H. Y., Huang, T. T., Wen, G. et al. (2022). Synthesis of dual pH- and temperature-sensitive poly (N-isopropylacrylamide-co-acrylic acid)/sewage sludge ash hydrogel with the simultaneously high performance of swelling and deswelling. *Polymers for Advanced Technologies, 33(1),* 235–245. DOI 10.1002/pat.5509.
38. Yang, J., Zhao, J. J., Han, C. R., Duan, J. F. (2014). Keys to enhancing mechanical properties of silica nanoparticle composites hydrogel: The role of network structure and interfacial interactions. *Composites Science and Technology, 95,* 1–7. DOI 10.1016/j.compscitech.2014.02.003.
39. Ganji, F., Vasheghani-Farahani, S., Vasheghani-Farahani, E. (2010). Theoretical description of hydrogel swelling: A review. *Iranian Polymer Journal, 19(5),* 375–398. DOI 10.3139/217.2330.
40. Mohammadi, N. S., Khiabani, M. S., Ghanbarzadeh, B., Mokarram, R. R. (2020). Improvement of lipase biochemical properties via a two-step immobilization method: Adsorption onto silicon dioxide nanoparticles and entrapment in a polyvinyl alcohol/alginate hydrogel-sciencedirect. *Journal of Biotechnology, 323,* 189–202. DOI 10.1016/j.jbiotec.2020.07.002.
41. Gharekhani, H., Olad, A., Mirmohseni, A., Bybordi, A. (2017). Superabsorbent hydrogel made of NaAlg-g-poly (AA-co-AAM) and rice husk ash: Synthesis, characterization, and swelling kinetic studies. *Carbohydrate Polymers, 168(1),* 1–13. DOI 10.1016/j.carbpol.2017.03.047.
42. Zeng, J., Cui, S., Wang, Q. Y., Chen, R. K. (2019). Multi-layer temperature-responsive hydrogel for forward-osmosis desalination with high permeable flux and fast water release. *Desalination, 459,* 105–113. DOI 10.1016/j.desal.2019.02.002.